

Experimental study of proton-induced nuclear reactions in ${}^{6,7}\text{Li}$

This article has been downloaded from IOPscience. Please scroll down to see the full text article.

2008 J. Phys. G: Nucl. Part. Phys. 35 014004

(<http://iopscience.iop.org/0954-3899/35/1/014004>)

View [the table of contents for this issue](#), or go to the [journal homepage](#) for more

Download details:

IP Address: 129.74.142.249

The article was downloaded on 09/05/2012 at 20:27

Please note that [terms and conditions apply](#).

Experimental study of proton-induced nuclear reactions in ${}^6,{}^7\text{Li}$

J Cruz^{1,2}, H Luis², M Fonseca², Z Fülöp³, G Gyürky³, F Raiola⁴,
M Aliotta⁵, K U Kettner⁶, A P Jesus^{1,2}, J P Ribeiro^{2,7}, F C Barker⁸
and C Rolfs⁴

¹ Dep. Física, Faculdade de Ciências e Tecnologia, Universidade Nova de Lisboa,
2829-516 Caparica, Portugal

² Centro de Física Nuclear da Universidade de Lisboa, 1649-003 Lisboa, Portugal

³ Atomki, Debrecen, Hungary

⁴ Institut für Experimentalphysik III, Ruhr-Universität Bochum, Germany

⁵ School of Physics, University of Edinburgh, UK

⁶ Fachhochschule Bielefeld, Germany

⁷ Dep. Física, Faculdade de Ciências, Universidade de Lisboa, 1749-016 Lisboa, Portugal

⁸ Dep. Theoretical Physics, Research School of Physical Sciences and Engineering,
The Australian National University, Canberra ACT 0200, Australia

E-mail: jdc@fct.unl.pt

Received 29 June 2007

Published 13 December 2007

Online at stacks.iop.org/JPhysG/35/014004

Abstract

The ${}^6\text{Li}(p,\alpha){}^3\text{He}$ and ${}^7\text{Li}(p,\alpha){}^4\text{He}$ reaction cross sections were obtained for $E = 90\text{--}580$ keV and $E = 90\text{--}1740$ keV, respectively. R -matrix and polynomial fits to the bare astrophysical S -factor confirmed, with improved accuracy, previous work data, yielding $S_b(0) = 3.52 \pm 0.08$ MeV b, and $55.6^{+0.8}_{-1.7}$ keV b for the ${}^6\text{Li}$ and ${}^7\text{Li}$ reactions, respectively. Therefore, the astrophysical consequences related to these two isotopes remain essentially unchanged. With the present work $S_b(E)$ data, a reanalysis of the low energy data for different environments— Li_2WO_4 insulator, Li metal, and PdLi_x alloys—confirms that the large electron screening effects can be explained by the plasma model of Debye applied to the quasi-free electrons in the metallic samples.

1. Introduction

Low-energy cross sections for reactions involved in the production and destruction of lithium isotopes give fundamental information for a number of still not completely solved astrophysical problems, e.g., the understanding of Big Bang nucleosynthesis and the so-called ‘lithium depletion’ either in the Sun or in other galactic stars.

The ${}^6\text{Li}(p,\alpha){}^3\text{He}$ and ${}^7\text{Li}(p,\alpha){}^4\text{He}$ reactions control the rate of ${}^6\text{Li}$ and ${}^7\text{Li}$ destruction, and the energy range of interest for both reactions in astrophysical scenarios is $E \lesssim 200$ keV.

The cross section, $\sigma(E)$, of a charged-particle-induced nuclear reaction is enhanced at sub-Coulomb energies ($E \lesssim 100$ keV for both Li reactions) by the electron clouds surrounding the interacting nuclides, with an enhancement factor over that for bare nuclei given by [1, 2]

$$f_{\text{lab}}(E) = \frac{\sigma_s(E)}{\sigma_b(E)} = E(E + U_e)^{-1} \exp[-2\pi\eta(E + U_e) + 2\pi\eta(E)], \quad (1)$$

where E is the centre-of-mass (CM) energy, $\eta(E)$ the Sommerfeld parameter and U_e the screening potential energy. Experimental studies of fusion reactions involving light nuclides have shown the expected exponential enhancement of the cross section at low energies [3–12]. However, the observed enhancements were for metals much larger than could be accounted for from available atomic-physics models [13]. These results were disturbing as, if we do not understand the effects of electron screening under laboratory conditions, we might also not understand fully the effects under astrophysical conditions. An explanation of the large screening was suggested by the Debye plasma model applied to the quasi-free metallic electrons [14, 15], which explained successfully the behaviour of U_e for the D(d,p)T reaction.

The Debye model predicts a linear scaling of U_e with the nuclear charge of the interacting nuclei, and that there is no isotopic dependence. These properties were verified with the ${}^7\text{Li}(\text{p},\alpha){}^4\text{He}$ and ${}^6\text{Li}(\text{p},\alpha){}^3\text{He}$ reactions in [16]. However, a precise quantification of this screening effect requires an equally accurate knowledge of the cross section at higher energies (where the electron screening effect is negligible). As the available data were not very precise and presented discrepancies [17], meaning that different data sets give different U_e values, a new study of both nuclear reactions at high energy, $E > 90$ keV, is reported alongside with a reanalysis of the low energy data. Details not contained here can be found in [18].

2. Equipment and procedures

The 2.5 MV Van de Graaff accelerator of the Instituto Tecnológico e Nuclear (ITN) in Sacavém provided H^+ , H_2^+ and H_3^+ beams (current on target < 200 nA) in the CM energy range $E = 80$ –1740 keV. The absolute beam energy is known to high precision leading to a maximum error in cross section of $\pm 0.65\%$. The beam passed through two collimators of $\phi = 2$ mm diameter at distances of 20.7 and 10.1 cm from the target holder. The targets ($\phi \approx 10$ mm) were installed in an electrically insulated cylindrical chamber, which served as a Faraday cup. The vacuum in the target area was 8×10^{-7} mbar.

For the measurement of angular distributions for ${}^7\text{Li}(\text{p},\alpha){}^4\text{He}$ at $E = 80$ –1740 keV, a ${}^7\text{Li}$ implanted into Al target with $(6.6 \pm 0.4) \times 10^{17}$ ${}^7\text{Li}$ cm^{-2} target was used with its normal oriented at 135° to the proton beam axis. Two movable Si detectors (50 mm^2 active area each) covered the angular range $\theta_{\text{lab}} = 84^\circ$ – 165° with an opening angle of 2° , and a precision of around 1° . Excitation functions for both Li reactions were measured concurrently for $E > 90$ keV with the same setup, at two fixed angles, $\theta_{\text{lab}} = 124^\circ$ and 145° . Three targets were used, two LiF targets ($(6.1 \pm 0.2) \times 10^{17}$ ${}^7\text{Li}$ cm^{-2} and $(9.0 \pm 0.4) \times 10^{17}$ ${}^7\text{Li}$ cm^{-2}) vacuum-evaporated on Ag and Cu backings (Li of natural isotopic composition: 92.58% ${}^7\text{Li}$, 7.42% ${}^6\text{Li}$) and the ${}^7\text{Li}$ implanted into Al target, which were positioned inside the target chamber with its normal antiparallel to the beam direction.

For an incident energy E_0 , a target thickness Δ , and an effective stopping cross section $\epsilon_{\text{eff}}(E)$ (all in CM system), the number of counts in a detector placed at θ_{lab} , $N(E_0, \theta_{\text{lab}})$, is related to the cross section, expressed in terms of the astrophysical S-factor:

$S(E) = \sigma(E)E \exp(2\pi\eta)$, via equation [2]

$$N(E_0, \theta_{\text{lab}}) = (1 + \delta)N_p \frac{\Omega_{\text{lab}}}{4\pi} \eta \int_{E_0 - \Delta}^{E_0} K_{\Omega}(E, \theta_{\text{lab}}) W(E, \theta) \frac{S(E) \exp(-2\pi\eta)}{E \epsilon_{\text{eff}}(E)} dE, \quad (2)$$

where $\delta = 1$ or 0 in the case of identical or non-identical ejectiles, N_p is the number of incident protons (measured by a charge integrator), and Ω_{lab} and η are the solid angle in the laboratory frame and efficiency of the detector, respectively ($\eta = 1$). The solid angle transformation between the laboratory and centre-of-mass systems is described by $K_{\Omega}(E, \theta_{\text{lab}})$ and the angular distributions are described by $W(E, \theta)$, where E and θ are CM coordinates. The ratio $N(E_0, \theta_{\text{lab}})/N_p$ was obtained by calculating the arithmetic mean (average) of up to four runs for each energy (this ratio remained stable to better than 5% for all energies).

The effective energy E within the target was derived from the incident energy of the ion beam and the energy loss of the beam in the target.

The quoted uncertainties for $S(E)$ arise from (1) the uncertainty in N_p . A precise charge evaluation was obtained from the simultaneously collected Rutherford backscattering spectroscopy (RBS) spectra for the LiF evaporated over the Ag self-supporting target. The uncertainty in N_p thus obtained is 4%. (2) The statistical uncertainty associated with $N(E_0, \theta_{\text{lab}})$ is $\delta N(E_0, \theta_{\text{lab}})/N_p = \max(\delta N_i, \delta N_e)$, with

$$\delta N_i = \left[\sum_{j=1}^n \frac{1}{y_j^2} \right]^{-1/2}, \quad \delta N_e = \left[\frac{\sum_{j=1}^n (y - y_j)^2 (1/\delta y_j)^2}{(n-1) \sum_{j=1}^n (1/\delta y_j)^2} \right]^{1/2}, \quad (3)$$

where the variable y stands for $N(E_0, \theta_{\text{lab}})/N_p$, and n for the number of runs at each energy. (3) A 5% uncertainty in stopping cross sections [19] affects not only $S(E)$ but also the effective energy, E . However, simulations show that the 5% uncertainty propagates into very small variations in energy ($<0.5\%$) and in $S(E)$ ($<3.7\%$; decreasing very fast with increasing energy). (4) The uncertainty associated with the measurement of the angular distributions, $W(E, \theta)$, is very small ($<0.2\%$). These uncertainties were added quadratically.

3. Results for ${}^7\text{Li}(\text{p}, \alpha){}^4\text{He}$

The observed angular distributions in CM coordinates are expressed in terms of Legendre polynomials,

$$W(E, \theta) = \sum_{\ell=0} A_{\ell}(E) Q_{\ell}(E) P_{\ell}(\cos \theta), \quad (4)$$

where Q_{ℓ} are the attenuation coefficients [18]. In the case of the ${}^7\text{Li}(\text{p}, \alpha){}^4\text{He}$ reaction, $W(E, \theta)$ is symmetrical around $\theta = 90^\circ$ and thus can be described by even Legendre polynomials. The deduced $A_2(E)$ and $A_4(E)$ coefficients are successfully parametrized by polynomial functions, as shown in the fits of figure 1 (the error shown represent statistical uncertainties only). The $A_2(E)$ values are in good agreement with previous works [3, 4] in the overlapping energy regions except around 900 keV, where our data are lower by $\approx 18\%$. For what concerns $A_4(E)$, it is not negligible for $E \gtrsim 1100$ keV. There are no previous data to compare with.

The S -factor obtained for $E = 90$ – 1740 keV is in good agreement with previous works [3, 4, 20], except at $E = 100$ – 400 keV, where our data are consistently below by 5%, and at $E \gtrsim 1200$ keV, where our data are slightly higher, as shown in figure 2 (the errors shown represent total uncertainties). However, these discrepancies between present and previous works, which are affected by large uncertainties as compared to our data, are compatible

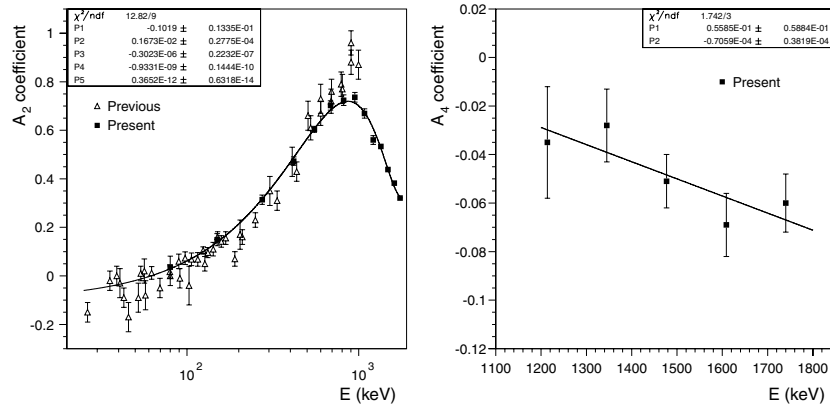


Figure 1. Left panel: energy dependence of the $A_2(E)$ coefficient in the angular distributions for the reaction ${}^7\text{Li}(p,\alpha){}^4\text{He}$ from the present work (\blacksquare). The solid curve represents a fourth-order polynomial fit to the present work. Data from previous works are also shown (Δ). Right panel: energy dependence of the $A_4(E)$ coefficient in the angular distributions for the reaction ${}^7\text{Li}(p,\alpha){}^4\text{He}$ from the present work (\blacksquare). The solid curve represents a linear fit to the data.

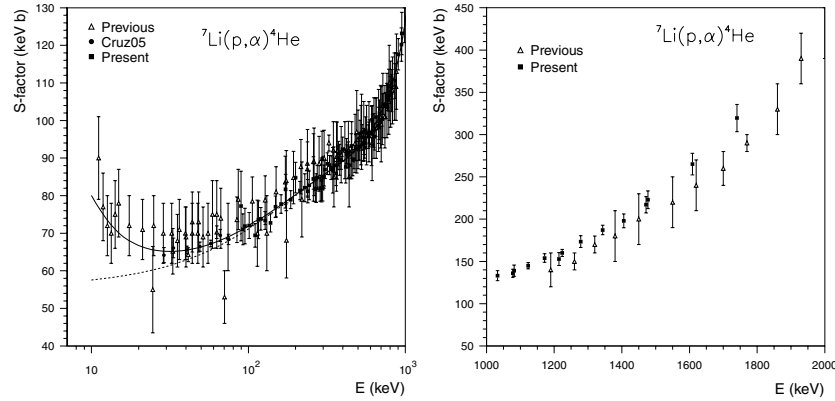


Figure 2. Previous (Δ), Cruz05 [16] (\bullet), and present (\blacksquare) data for the $S(E)$ factor of the ${}^7\text{Li}(p,\alpha){}^4\text{He}$ reaction as a function of the energy (left panel: $E \leq 1000$ keV; right panel: $E \geq 1000$ keV). The solid curve is an R -matrix best fit to present + [16] data which includes the bare $S(E)$ factor (dotted curve) and the electron screening with the U_e value given in the text.

within errors. For the ${}^6\text{Li}(p,\alpha){}^3\text{He}$ reaction, which was measured concurrently with the ${}^7\text{Li}(p,\alpha){}^4\text{He}$ reaction, no shift is observed (figure 3). The lower uncertainties obtained in the present work produce more accurate fits, performed with the function $S(E) = f_{\text{lab}} S_b(E)$, for both Li reactions. The present work data points alongside the $S(E)$ values measured for the Li_2WO_4 target [16] were fitted using a four 2^+ -level R -matrix formalism [17] to describe the bare component of $S(E)$ in the energy range from $E = 29$ –1100 keV. In addition, our results for the angular distribution coefficient A_2 also entered the fit. The results are shown in figure 2(a), with $S_b(0) = 55.6^{+0.8}_{-1.7}$ keV b, and $U_e = 237^{+133}_{-77}$ eV, which are within the range of values published in the literature [12, 17], $S_b(0) = 55$ –67 keV b, $U_e = 134$ –330 eV, and consistent with the atomic adiabatic limit $U_e = 186$ eV [13].

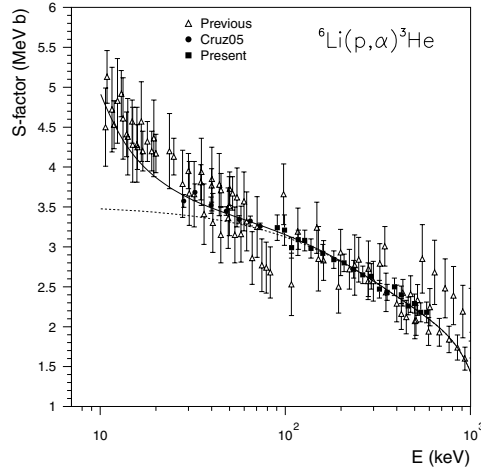


Figure 3. Previous (Δ), Cruz05 [16] (\bullet), and present (\blacksquare) data for the $S(E)$ factor of the ${}^6\text{Li}(p,\alpha){}^3\text{He}$ reaction as a function of the energy. The solid curve is a fit with a third-order polynomial function to data from present work, [16, 22] which includes the bare $S(E)$ factor (dotted curve) and the electron screening with the U_e value given in the text.

4. Results for ${}^6\text{Li}(p,\alpha){}^3\text{He}$

Even though there is some dispersion on previous works data [4, 21–23], our values are in good agreement with the overall data, as shown in figure 3 (the error shown represent total uncertainties).

For the ${}^6\text{Li}(p,\alpha){}^3\text{He}$ reaction, an R -matrix fit requires contributions from both positive- and negative-parity levels of ${}^7\text{Be}$, formed by s - and p -wave protons, respectively, in order to fit the dominant angular distribution coefficient A_1 [17]. The p -wave negative-parity levels nearest to the ${}^6\text{Li} + p$ threshold are the two broad $5/2^-$ levels at 6.73 and 7.21 MeV with well-known properties. Shell-model calculations predict the lowest positive-parity level to be $1/2^+$. From $5/2^-$ and $1/2^+$ levels, however, it is not possible to obtain any contribution to A_1 . A nonzero A_1 requires $1/2^-$ or $3/2^-$ levels together with the $1/2^+$ level, or $3/2^+$, $5/2^+$ or $7/2^+$ levels together with the $5/2^-$ levels, and the properties of such additional levels are too uncertain to make feasible an R -matrix fit to A_1 . So, as in [17], we make a polynomial fit to the $S(E)$ data, varying the polynomial parameters and the screening potential energy separately, using the present work and [22] data, for the energy range $E = 90$ – 1000 keV, and the Li_2WO_4 data for $E < 83$ keV [16]. The fits results, shown in figure 3, are $S_b(0) = 3.52 \pm 0.08$ MeV b, and $U_e = 273 \pm 111$ eV, which are also within the range of values published in the literature [4, 11, 17], $S_b(0) = 3.00$ – 3.56 MeV b, $U_e = 260$ – 470 eV, and again consistent with the atomic adiabatic limit $U_e = 186$ eV [13].

5. Discussion

The ${}^7\text{Li}(p,\alpha){}^4\text{He}$ angular distributions measurements show that for $E \gtrsim 1100$ keV the $A_4(E)$ coefficient is not negligible, so f -wave protons, in addition to p -wave protons, should be taken into account for the theoretical description of the entrance channel of this reaction in this energy range. This $A_4(E)$ behaviour is, to our knowledge, reported for the first time.

The present work has confirmed, with improved accuracy, the absolute cross sections reported by previous authors for both Li reactions. Therefore, the astrophysical consequences related to these two isotopes remain essentially unchanged.

With the new $S_b(E)$ data obtained in this work, a reanalysis of the low energy data presented in [16] gives, for the ${}^7\text{Li}(p,\alpha){}^4\text{He}$ reaction, $U_e = 1180 \pm 60$ eV (Li metal), and $U_e = 3680 \pm 330$ eV ($\text{Pd}_{94.1\%}\text{Li}_{5.9\%}$). For the ${}^6\text{Li}(p,\alpha){}^3\text{He}$ reaction, we get $U_e = 1280 \pm 70$ eV (Li metal), and $U_e = 3710 \pm 185$ eV ($\text{Pd}_{94.1\%}\text{Li}_{5.9\%}$). These U_e values are ≈ 100 eV lower, but compatible within errors to the values reported in [16]. So, these new results confirm the conclusions presented in [16], i.e., the large U_e values can be explained by the plasma model of Debye applied to the quasi-free electrons in these metallic samples.

Acknowledgment

This work was supported by Portugal (POCTI-FNU/45092/2002), BMBF (05CL1PC1), DFG (Ro429/31,436Ung113).

References

- [1] Assenbaum H J, Langanke K and Rolfs C 1987 *Z. Phys. A* **327** 461
- [2] Rolfs C and Rodney W S 1989 *Cauldrons in the Cosmos* (Chicago, IL: University of Chicago Press)
- [3] Rolfs C and Kavanagh R W 1986 *Nucl. Phys. A* **455** 179–88
- [4] Engstler S, Raimann G, Angulo C, Greife U, Rolfs C, Schröder U, Somorjai E and Kirch B 1992 *Z. Phys. A* **342** 471–82
- [5] Greife U, Gorris F, Junker M, Rolfs C and Zahnw D 1995 *Z. Phys. A* **351** 107
- [6] Zahnw D *et al* 1997 *Z. Phys. A* **359** 211
- [7] Czerski K, Hulke A, Biller A, Heide P, Hoeft M and Ruprecht G 2001 *Europhys. Lett.* **54** 449
- [8] Lattuada M, Pizzone R G, Typel S, Figuera P, Miljanic D, Musumarra A, Pellegriti M G, Rolfs C, Spitaleri C and Wolter H H 2001 *Astrophys. J.* **562** 1076
- [9] Raiola F *et al* 2002 *Eur. Phys. J. A* **13** 377
- [10] Kasagi J 2002 *J. Phys. Soc. Japan* **71** 2881
Kasagi J 2004 *J. Phys. Soc. Japan* **73** 608
- [11] Tumino A 2003 *Phys. Rev. C* **67** 065803
- [12] Descouvemont P, Abderrahim A, Angulo C, Coc A and Vangioni-Flam E 2004 *At. Data Nucl. Data Tables* **88** 203–36
- [13] Bracci L, Fiorentini G, Melezhik V S, Mezzorani G and Quarati P 1990 *Nucl. Phys. A* **513** 316
- [14] Raiola F *et al* 2004 *Eur. Phys. J. A* **19** 283
- [15] Raiola F *et al* 2005 *J. Phys. G: Nucl. Part. Phys.* **31** 1141
- [16] Cruz J *et al* 2005 *Phys. Lett. B* **624** 181–85
- [17] Barker F C 2002 *Nucl. Phys. A* **707** 277–300
- [18] Cruz J 2006 *PhD Thesis* New University of Lisboa
- [19] URL of SRIM: www.srim.org
- [20] Cassagnou Y, Jeronimo J M, Mani G S, Sadeghi A and Forsyth P D 1963 *Nucl. Phys.* **41** 176
- [21] Marion J B, Weber G and Mozer F S 1956 *Phys. Rev.* **104** 1402
- [22] Elwyn A J *et al* 1979 *Phys. Rev. C* **20** 1984
- [23] Shinozuka T, Tanaka Y and Sugiyama K 1979 *Nucl. Phys. A* **326** 47